

RESEARCH ARTICLE

Open Access



# Alginate-coated perlite beads for the efficient removal of methylene blue, malachite green, and methyl violet from aqueous solutions: kinetic, thermodynamic, and equilibrium studies

Şerife Parlayici

## Abstract

Environmental pollution has been increasing recently due to industrialization. Many industries use dyestuffs to color their products. This work investigates the adsorption of methylene blue (MB), malachite green (MG), and methyl violet (MV) on alginate-coated perlite beads (AP). AP was prepared by a sol-gel process. The removal of MB, MG, and MV from aqueous solutions by AP as an adsorbent was tested by using a batch-type model. In order to prove the effectiveness of the study, it has been tried to obtain optimum efficiency at optimum level by working depending on mixing time (minutes), initial dye concentration (ppm), adsorbent dose (mg/L), pH, and temperature (°C). The results showed that the MB, MG, and MV adsorption process reached equilibrium within a 60-min period for AP. It has been found that the amount of adsorbed dyestuff increases with the initial dye concentration, the pH of the solution. Thermodynamic activation parameters were calculated from experimental data at different temperatures. The AP was characterized by Fourier Transform Infrared Spectroscopy (FT-IR) before and after MB, MG, and MV adsorption. The equilibrium adsorption data were described by Langmuir, Freundlich, Scatchard, Temkin and D-R isotherms. The modified Langmuir isotherm was applied to explain the experimental adsorption, and the greatest MB, MG, and MV adsorption capacity of the AP reached to 104.1, 74.6, and 149.2 mg/g, respectively. The pseudo-first and pseudo-second-order equations were used to evaluate the kinetic data, and the constants are determined. The best correlation coefficients were well described using the pseudo-second-order kinetic model. As a result, AP has claimed the possibility as an adsorbent for MB, MG, and MV removal from dilute aqueous solutions.

**Keywords:** Perlite, Alginate, Adsorption isotherms, Methylene blue, Malachite green, Methyl violet

## Introduction

Considering the limited availability of water resources in the world, the problem of water pollution is one of the most important environmental problems in our day. Dyestuffs are found in the wastes of many industries such as textile, paper, plastic, and dyestuff. These dyes cause significant pollution (Crini and Badot 2008). Organic and biodegradable wastes and dyes are exposed to the attack of bacteria when given to surrounding waters. Bacteria decompose these organic structures and use

oxygen dissolved in the water, which is the source of life for the living things in the water. Thus, the dissolved oxygen concentration in the water is reduced. Most of the microbiological life that should be in the aquatic environment needs oxygen dissolved in water. In the case of organic substances thrown into the water, all dissolved oxygen is used. Thus, the aquatic environment can be an oxygen-free environment for living things. In this case, the ecological balance of living things in the water is disturbed and their living life is greatly damaged. Painted wastewater causes significant environmental problems due to their toxic effects on aquatic life and decreasing light permeability and photosynthetic activity in aquatic

Correspondence: [serife842@hotmail.com](mailto:serife842@hotmail.com)

Department of Chemical Engineering, Faculty of Engineering and Natural Sciences, University of Konya Technical, Campus, 42071 Konya, Turkey



© The Author(s). 2019 **Open Access** This article is distributed under the terms of the Creative Commons Attribution 4.0 International License (<http://creativecommons.org/licenses/by/4.0/>), which permits unrestricted use, distribution, and reproduction in any medium, provided you give appropriate credit to the original author(s) and the source, provide a link to the Creative Commons license, and indicate if changes were made.

life. For some dyestuffs, the presence of a small amount of dye in the water, which is less than 1 mg/L, causes image pollution (Crini 2006). Color creates a problem in terms of esthetics and also limits the possibility of reuse of water. Even at a concentration of 1 mg/L, it disturbs drinking water and makes consumption impossible. Dyestuffs have a negative effect on the kidneys, reproductive system, lungs, brain, and central nervous system (Salleh et al. 2011). Most paints can cause serious health problems such as skin allergies, cancer, and mutation in humans. Therefore, dye removal from wastewater is necessary for human and environmental health.

Methylene blue dye is widely used in the textile, leather, paper, wood, and plastic industries. It can cause eye burns in human and animals and permanent damage to eyes. In addition, it can cause nausea, vomiting, excessive sweating, short-term mental confusion, and rapid and difficult breathing (Theydan and Ahmed 2012). Malachite green is widely used in silk, wool, leather, cotton, and paper in dyeing. However, it is environmentally permanent and toxic to aquatic and terrestrial animals. Methyl violet is widely used in textile industries and to give purple color to paints and printing ink (Bouasla et al. 2010). Therefore, the release of this dye into the environment is a matter of great concern, and its oxidative degradation is highly required. It causes various diseases (carcinogen, mutagen, and mitotic poison). Considering the potential harmful effects of MB, MG, and MV dyestuffs, the importance of removing dyestuffs from wastewaters is more evident.

Therefore, wastewater generated from pollution sources should be treated before being discharged to the environment and reduced below the permissible pollution values according to various water standards. Cleaning industrial wastes; different methods are used depending on the origin of the wastes, type of use, purpose of use and local resources. Many biological-, physical-, and chemical-based methods are used for dye removal. The methods for removing dyestuff from water are anaerobic treatment, flocculation/coagulation, membrane filtration, adsorption, biosorption, photocatalysis, electrocoagulation, and ion exchange (Papegowda and Syed 2017; Puri and Sumana 2018; Yi et al. 2015; Xu et al. 2018). Especially, one of the methods with high yield efficiency in the increase of dyed wastewater is adsorption. Among these, adsorptions from the aqueous system have been widely used and an attractive method for the removal of pollutants from aqueous media. For this target, a number of adsorbents have been employed for different types of pollutants.

Recently, many investigators have been carried out on the effective removal of MB, MG, and MV from synthetic wastewater using adsorbents such as chitin/clay microspheres (Xu et al. 2018), calcium alginate/acid-activated organobentonite composite beads

(Djebri et al. 2016), natural clay of Agadir region (Bentahar et al. 2018), chitosan/cellulose beads (Vega-Negron et al. 2018), graphene oxide intercalated montmorillonite nanocomposites (Puri and Sumana 2018), zeolite nanostructures (Abdelrahman 2018), sodium alginate-based organic/inorganic superabsorbent composite (Thakur et al. 2016), alginate/natural bentonite composite beads (Oussalah et al. 2019), and magnetic calcium alginate beads (Asadi et al. 2018).

The most important criterion in the selection of adsorbents to be used in the adsorption process is that it is easy to find, cheap, and reusable. On the other hand, one of the most economical methods used in the removal of dyestuffs is the adsorption of beads from the biopolymer as adsorbents. In the study, perlite natural minerals were added to the structure of biopolymers in the production of composite beads. Perlite is an ideal mineral for the construction of composite microspheres due to its porous structure, thermal durability, large surface area, and cheap properties.

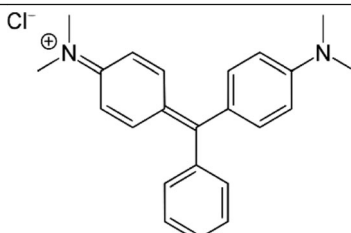
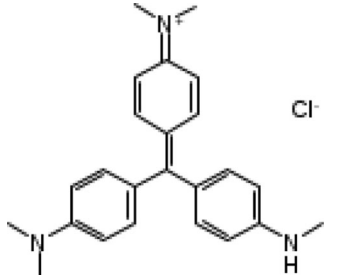
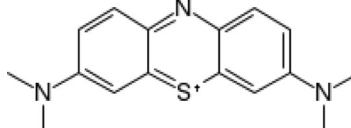
The main subject of this study is the synthesis of composite microspheres for dye removal with alginate-coated perlite beads characterized using FT-IR. In the literature researches, it has been observed that the use of clays, perlite, and zeolite as adsorbent material has been the subject of curiosity in recent years and it has been started to be investigated extensively. However, alginate-coated perlite composites with MB, MG, and MV were not studied at all. In this study, it was observed that the removal capacity of MB, MG, and MV of composite beads was much higher than that of alginate-coated perlite beads and untreated perlite. Various adsorption parameters such as adsorbent amount, equilibrium time, temperature, pH, and concentration of MB, MG, and MV dye solutions at initial stage were applied, and the morphological behavior before and after interactions was investigated. Moreover, kinetics (pseudo-first and pseudo-second order), sorption equilibrium isotherms (Langmuir, Freundlich, Scatchard, Temkin, and D-R models), and thermodynamic studies were applied in this work. The search for new alternative, cheap, eco-friendly, and efficient adsorbents to replace the commercially available adsorbents is ongoing.

## Materials and methods

### Materials

Sodium alginate powder was obtained from Sigma-Aldrich, and raw expanded perlite (P) was purchased from PerSa Company in Konya, Turkey. The expanded perlite used is in the range of 0.35–0.60–0  $\mu\text{m}$ . Methylene blue, malachite green, and methyl violet referred to as MB, MG, and MV were purchased from Acros Organics (Table 1). Dye solution was prepared by dissolving the calculated powder dye in distilled water with different

**Table 1** Physicochemical properties of dyes (malachite green, methyl violet, and methylene blue)

Commercial name	Structural formula	$\lambda_{\max}$ (nm)	Molecular formula	M (g mol <sup>-1</sup> )
Malachite green oxalate		617	C <sub>23</sub> H <sub>25</sub> N <sub>2</sub> · 1/2C <sub>2</sub> H <sub>2</sub> O <sub>4</sub> · C <sub>2</sub> HO <sub>4</sub>	463.51
Methyl violet 2B		579	C <sub>24</sub> H <sub>28</sub> ClN <sub>3</sub>	393.96
Methylene blue hydrate		664	C <sub>16</sub> H <sub>18</sub> ClN <sub>3</sub> S · xH <sub>2</sub> O	319.85

required concentrations. All related chemicals used in the experiments were of analytical grade, and distilled water was used for the preparation of the necessary solutions. CaCl<sub>2</sub>, NaOH, and HCl solutions were obtained from Merck Company. The pH of solutions was adjusted by adding NaOH and HCl. Deionized (DI) water was used throughout this study.

#### Apparatus

A pH meter (Orion 900S2) with glass electrode and internal reference electrode was used for pH measurements. Thermostated shaker of GFL 3033 model was used for mixing of the bulk solutions in adsorption experiments. UV-visible spectrophotometer (Schmadzu UV-1700) was used for the determination of MB, MG, and MV content in standard and treated solutions. The FT-IR spectrum was recorded by a Bruker VERTEX 70 FT-IR spectrometer.

#### Preparation of alginate coated perlite beads

Suspension of 5% (w/v) of sodium alginate was prepared by mixing the sodium alginate powder with distilled water. This suspension was dissolved in distilled water at 2 h. The suspension of perlite 5% (w/v) was prepared and dispersed in distilled water. Perlite suspension was added to the alginate gel in the form of 1/1 mass ratio (perlite/alginate), and the solution was then stirred with a magnetic stirrer for 5 h to form a homogenous solution. After that, the solution was kept in a dark

medium for overnight. The resulting slurry was added dropwise, by using a 5-mL syringe (needle size 0.6 mm) from a 5-cm height, into a 0.6 M CaCl<sub>2</sub> solution (1 mL gel/5 mL CaCl<sub>2</sub>) under constant stirring at 100 rpm. After that, the AP beads were kept in a dark medium for overnight. The AP beads formed, and the slurry was filtrated and washed with distilled water until neutral (Fig. 1). They were then dried at ambient temperature.

#### Batch adsorption and kinetics models

Batch adsorption experiments were performed with the different amounts of AP in a 100-mL glass bottle. AP was weighed in the sensitive balance, then placed in 100-mL flasks, and then the dye solution was added to each of the test samples. The prepared samples were placed in the shaker. The shaker was run at 25, 35, 45, and 55 °C at 150 rpm at the end of agitation times. All experimental results were checked to remove the errors by blank tests in which no adsorbent was added into the dye solution. Kinetic and equilibrium experiments were conducted for 5–240 min. The samples were tested two times to ascertain the accuracy, reliability, and reproducibility of the data obtained from experimental results. After equilibrium was reached, the filtrate was measured using UV-vis spectrophotometer (Schmadzu UV-1700). The adsorption capacity at time *t*, *q<sub>t</sub>* (mg/g), was obtained as Eq. (1) (Pehlivan et al. 2009):

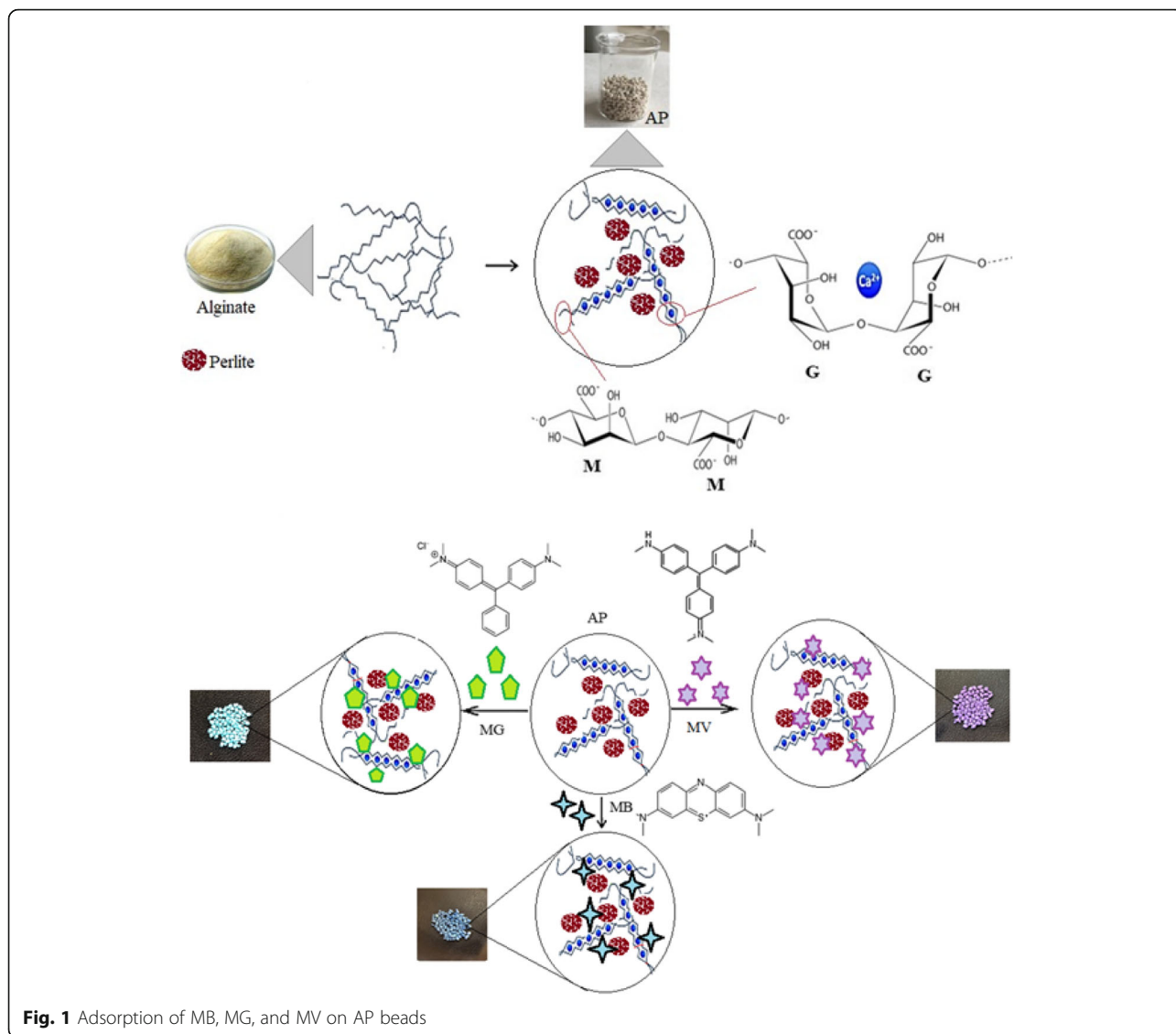


**Fig. 1** Adsorption of MB, MG, and MV on AP beads

$$q_e = \frac{C_i - C_f}{m} \times V \tag{1}$$

where  $q_e$  is the adsorbed dye (mg/g adsorbent) on the adsorbents,  $m$  is the mass of AP (g),  $V$  is the volume of dye solution (L),  $C_i$  is initial dye concentration (mmol/L), and  $C_f$  is the dye concentration (mmol/L) at any time.

The percent adsorption of dye can be demonstrated as follows (Eq. (2)):

$$\% \text{Adsorption} = \frac{C_i - C_f}{C} \times 100 \tag{2}$$

Adsorption isotherms have an important place in the design of adsorption process. Langmuir isotherm presents a single-layer homogeneous adsorption (Langmuir

1916). The Freundlich isotherm is defined for reversible and non-ideal adsorption, which is not limited to monolayer formation. According to Freundlich, the adsorbing areas on the surface of an adsorbent are heterogeneous. It is formed of different types of adsorbing areas. Temkin isotherm assumes that the decrease in sorption temperature is linear rather than logarithmic, unlike the Freundlich equation. The adsorption is characterized by uniform distribution of the binding energies until they reach the maximum binding energy (Temkin 1940). The average adsorption energy calculated by the D-R isotherm allows us to be informed about the physical and chemical properties of the adsorbing area (Dąbrowski 2001). The D-R isotherm is used to explain the adsorption processes in the same type of porous structures. There are various kinetic models that characterize the adsorption process, i.e., to determine what kind of

mechanism plays a role in the adsorption of the dyestuff to the adsorbent surface. The pseudo-first-order and pseudo-second-order kinetic models were studied.

## Results and discussion

### Characterization of the beads

The FT-IR spectra of AP were measured within the range of 500–4000  $\text{cm}^{-1}$  and are displayed in Fig. 2. Some changes in the characteristic peaks ranging from 900 to 3600  $\text{cm}^{-1}$  and some visible shifts of peak locations of AP were observed before and after adsorption of dyestuff. The evidence for the presence of alginate comes from the appearance of two peaks at 1598  $\text{cm}^{-1}$  due to asymmetric stretching vibration and at near 1428  $\text{cm}^{-1}$  due to asymmetric COO<sup>-</sup> stretching vibration (Mohammadi et al. 2014; Abdelrahman and Hegazey 2019). Mannuronic and gluronic acid in the structure of alginate or in other words the polysaccharide structure were represented by 819  $\text{cm}^{-1}$  band. In the FT-IR spectrum, bands at 3376 and 3367  $\text{cm}^{-1}$  present vibration of -OH groups in the water molecules connected to the Si-O-Al surface by weak hydrogen bond (Nassar et al. 2017; Abdelrahman et al. 2018). Si-O vibration of

Si-O-Si groups in perlite was observed near 1079  $\text{cm}^{-1}$  (Xu et al. 2018; Nassar and Abdelrahman 2017; Abdelrahman 2018). Changes in peak frequencies in FT-IR spectra correspond to changes in the energy of the functional group. Therefore, changes that occur after adsorption and changes in the formation or disappearance of new peaks are indications that the peaks are involved in the adsorption and the dyes are added to the structure. In the pre-adsorption and post-adsorption FT-IR analysis of the dyestuff of the AP, for MB prior to adsorption, it was observed that the peak in 1598.70  $\text{cm}^{-1}$  shifted to 1590.99  $\text{cm}^{-1}$ , the peak in 1428.99  $\text{cm}^{-1}$  to 1415.50  $\text{cm}^{-1}$ , and the peak in 1014.37  $\text{cm}^{-1}$  to 1024.02  $\text{cm}^{-1}$ ; for MG, the peak in 1598.70  $\text{cm}^{-1}$  to 1589.06  $\text{cm}^{-1}$ , the peak in 1428.99  $\text{cm}^{-1}$  to 1417.42  $\text{cm}^{-1}$ , and the peak in 1014.37  $\text{cm}^{-1}$  to 1024.02  $\text{cm}^{-1}$ ; and for MV, the peak in 1598.70  $\text{cm}^{-1}$  to 1589.98  $\text{cm}^{-1}$ , the peak in 1428.99  $\text{cm}^{-1}$  to 1425.14  $\text{cm}^{-1}$ , and the peak in 1014.37  $\text{cm}^{-1}$  to 1024.02  $\text{cm}^{-1}$  peak after adsorption and then decreased. Also, it is seen that the band around 3376.75  $\text{cm}^{-1}$  in its spectrum shrinks after adsorption of all three dyes. The reason for this sharp decline is thought to be due to ionic interactions between the -OH groups in the

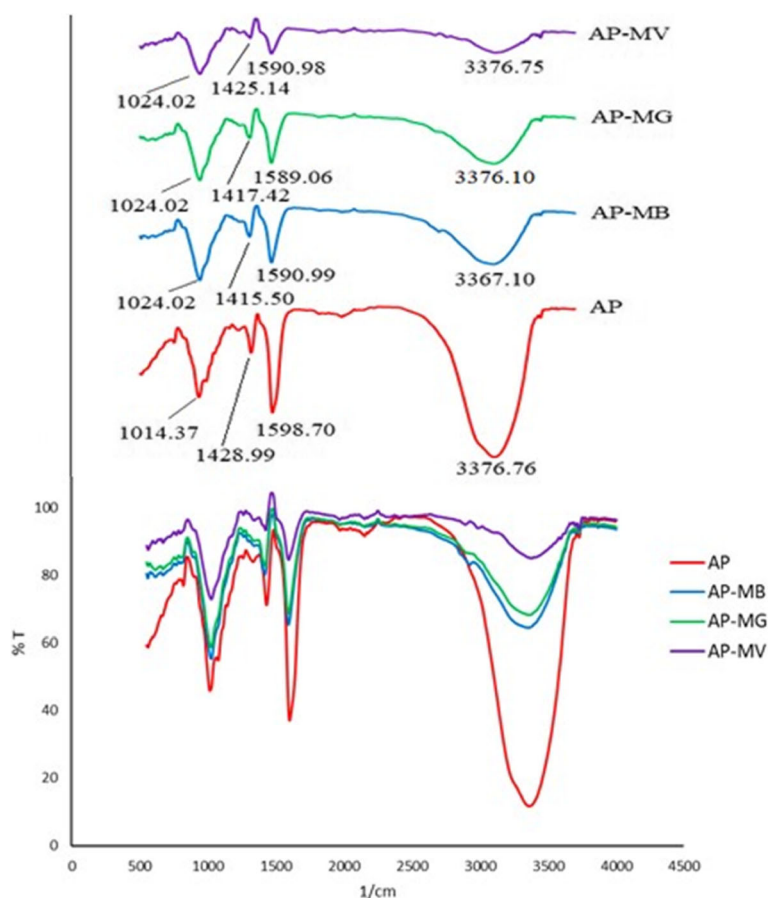


**Fig. 2** FTIR spectrum of AP before and after adsorption of MB, MG, and MV

structure and the dyestuffs, where the shift of the bands may indicate that these functional groups interact with the MB, MG, and MV molecules (Xu et al. 2011).

**Effect of adsorbent dosage**

The amount of dyestuff adsorption was investigated by adsorption experiments with different adsorbent amount values (0.5–4.0 g/L for P, 0.5–2.5 g/L for AP). The effect of the amount of adsorbent dosage on the percentage of dyestuff removal is shown in Fig. 3b, d, and the effect on the adsorption capacity is given in Fig. 3a, c. As shown in the graph, for the removal of all three dyestuffs, the adsorbent amount increases while the adsorption of dyes increases, reaching a plateau value after a certain value. After this plateau value, the increase in the amount of adsorbent does not significantly affect the adsorption. After this point, because of the fact that the adsorption event was an equilibrium event, there was no significant effect of increasing the amount of adsorbent on the dye removal. The increase in percent removal of adsorbate ions with increase in the adsorbent dose could be attributed to greater availability of adsorption sites. At equilibrium, the percent removal became constant probably because of the saturation of the available adsorption sites. Equilibrium was attained at an adsorbent dosage of 2 g/L for P and 1 g/L for AP. Another result of Fig. 3 was that with the increasing amount of AP and P, the adsorption

capacity ( $q_e$ ) decreased significantly. As the amount of adsorbent increases, the percentage of dyestuff removal increases, but the adsorption capacity decreases. The possible cause of this situation is the existence of a large number of empty active centers in the environment compared to fixed dye concentration. It was believed that the adsorbate particles were massive, decrease the surface area of the adsorbent, and prolong the path in the diffusion step (Ghaedi et al. 2014).

**Effect of contact time**

When examined in Fig. 4, it was observed that adsorption was very rapid in all of the different initial concentration studies. The reason for this was that initially the appropriate surface area for adsorption was high. Over time, these places begin to fill up and the rate of adsorption slows down as the equilibrium was approached. As can be seen from the figures and tables, in almost all of the adsorption studies of different initial concentration P and AP adsorbents in MB, MG, and MV adsorbents after 240 min, more than half of the adsorbed amount was adsorbed in the first 30 min. For MB, MG, and MV adsorption with P, in the 60th minute, the adsorption was gradually increasing and it reaches equilibrium in the 120th minute. For MB, MG, and MV adsorption with AP, the adsorption at the 30th minute increases

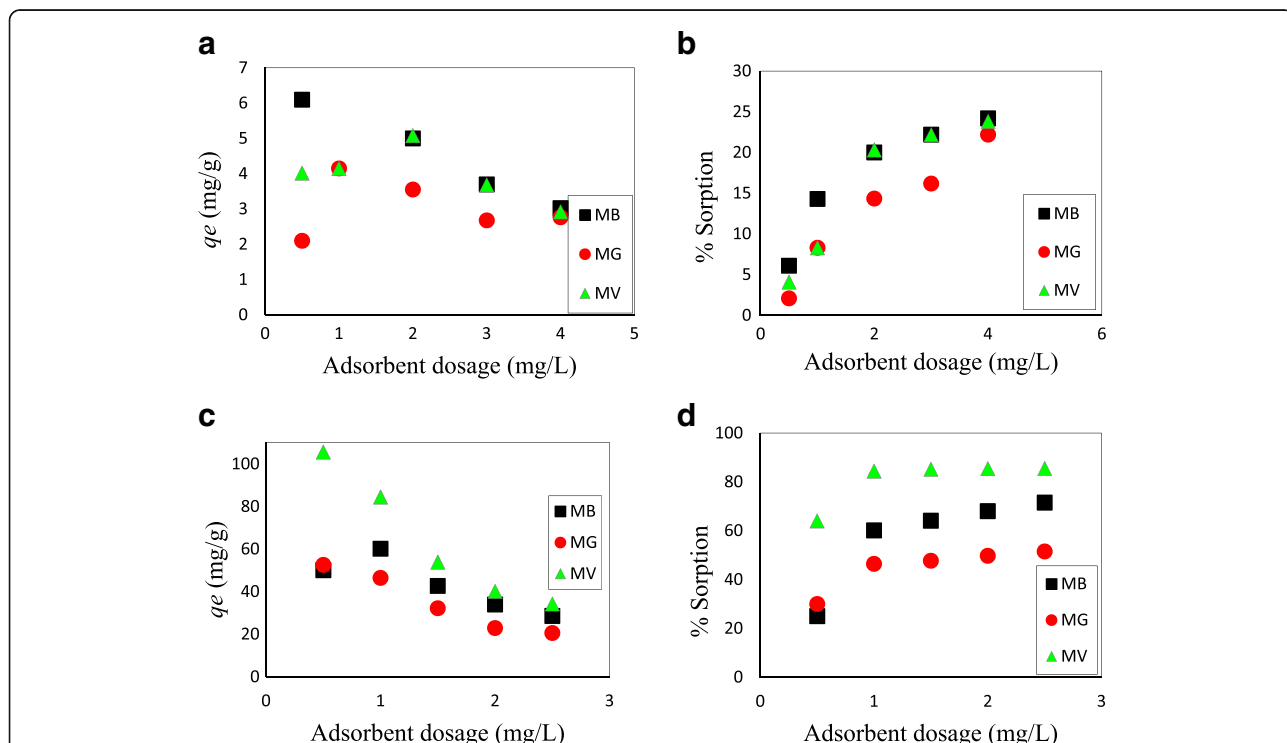


**Fig. 3** Effect of adsorbent dosage. **a** P- $q_e$ . **b** P-% sorption. **c** AP- $q_e$ . **d** AP-% sorption (adsorption conditions: concentration of cationic dye 50 ppm, solution pH, contact time 120 min, and temperature  $25 \pm 1$  °C for P and concentration of cationic dye 100 ppm, solution pH, contact time 60 min, temperature  $25 \pm 1$  °C for AP)

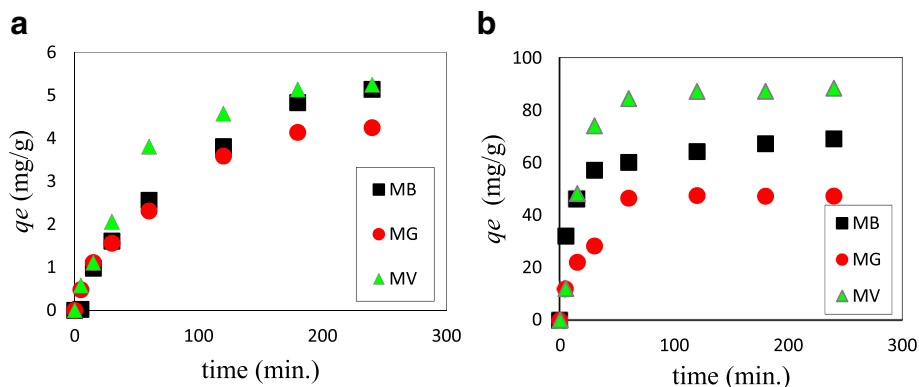


**Fig. 4** Effect of contact time on the adsorption of dye by P (a) and AP (b) (adsorption conditions: concentration of cationic dye 50 ppm, solution pH, adsorbent amount 2 g/L, and temperature  $25 \pm 1^\circ\text{C}$  for P and concentration of cationic dye 100 ppm, solution pH, adsorbent amount 1 g/L, and temperature  $25 \pm 1^\circ\text{C}$  for AP)

gradually and reaches equilibrium at the 60th minute. For all dyes, the balance duration was 60 min for AP and 120 min for P. In addition, for all of the adsorption of MB, MG, and MV, it was observed that AP had more adsorption capacity compared to P.

**Effect of pH**

The initial pH of the media is very important in terms of adsorption processes and adsorption capacity. The

starting pH of the medium was changed in the range of 2–10. As the pH is increased from 2 to 8 for three dyestuffs, the concentration of dyestuffs held and the capacity of P and AP to reduce dyestuffs were increased (Fig. 5). This is an expected result because the MB, MG, and MV dyes are cationic in character.

The point of zero charge ( $\text{pH}_{\text{PZC}}$ ) of AP and P was found to be at pH 6.1. Using the concept of  $\text{pH}_{\text{PZC}}$ , the surface of AP will be predominant negatively charged

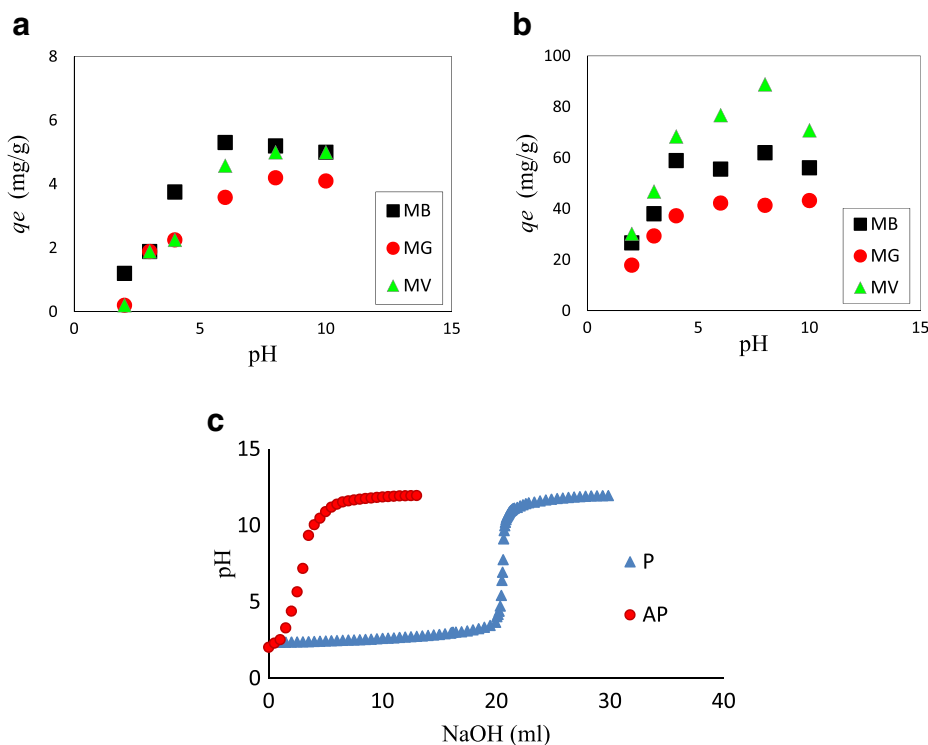


**Fig. 5** Effect of pH on the adsorption of dyes using a P and b AP. c  $\text{pH}_{\text{PZC}}$  of P and AP (adsorption conditions: concentration of cationic dye 50 ppm, adsorbent amount 2 g/L, contact time 120 min, and temperature  $25 \pm 1^\circ\text{C}$  for P and concentration of cationic dye 100 ppm, adsorbent amount 1 g/L, contact time 60 min, and temperature  $25 \pm 1^\circ\text{C}$  for AP)

when solution pH > 6.1, while predominant positively charged when pH < 6.1. The adsorption of cationic dyestuffs (MB, MG, and MV) by P and AP is more pronounced in the pH > pHPZC. Considering the adsorption between the negatively charged surface and the cationic dyestuff, the excess H<sup>+</sup> ions in the environment at acidic pH values settled at the appropriate centers for adsorption on the adsorbent and prevented adsorption of the cationic dyestuffs. At low pH values, therefore, the removal of ions from the aqueous solution is difficult due to the electrostatic propulsion between the positively charged adsorbent surface and the dyestuff. As can be seen from Fig. 5, a point is reached where the surface load is zero (pH range) with increasing pH. After this point, with the increase in pH value, P and AP surfaces have a negative character and MB, MG, and MV adsorption are increased. For this reason, adsorption becomes

more in high pH conditions and optimum pH value was found as 6. Similar results are available in the literature (Thakur et al. 2016). The original pH values of the adsorbates are MB 6.8, MG 6.4, and MV 6.7, and they are close to their maximum adsorption pH (pH = 6), which is also advantageous in terms of cost.

**Adsorption isotherms**

Dyestuff adsorption with different concentrations plays an important role in determining the adsorption capacity of the adsorbent (Fig. 6) (Gobi et al. 2011). At higher initial concentrations of dyestuffs, the mass transfer resistance between the solid surface and the solution was more easily overcome. With the increasing concentration of dyestuff, empty active centers on the surface of the adsorbent were filled rapidly. As the initial concentration increased, the adsorption capacity increased.

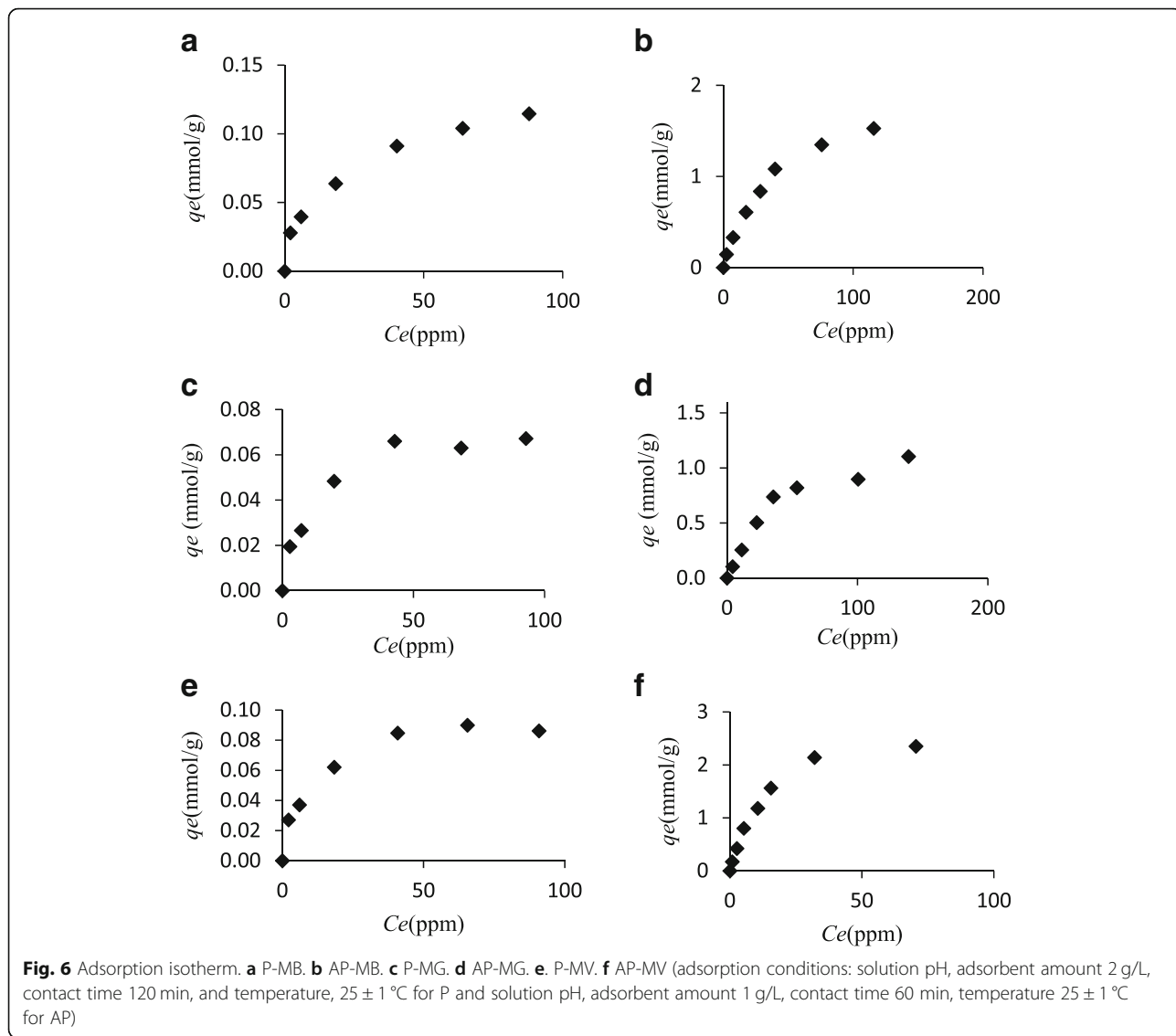


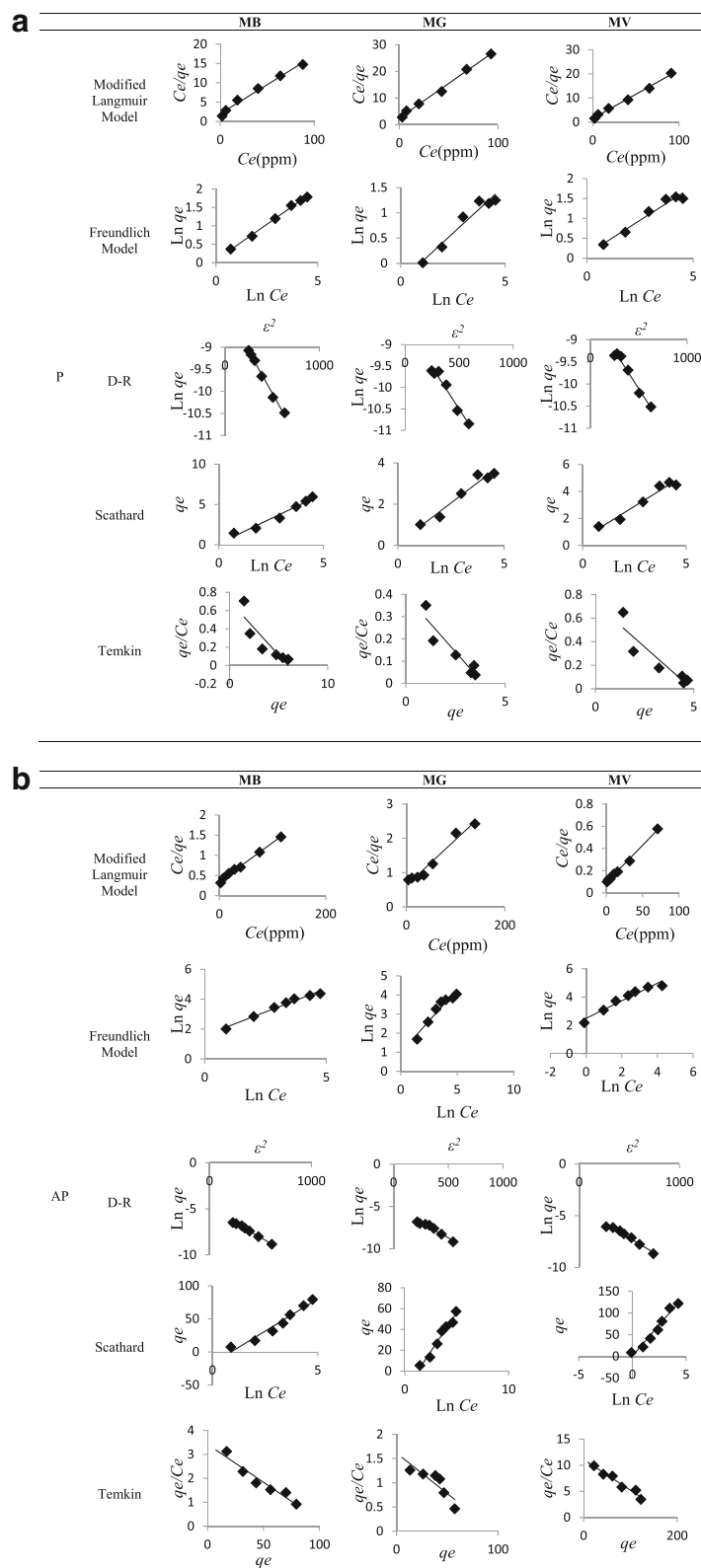


Table 2 shows the results of modified Langmuir, Freundlich, Scatchard, D-R, and Temkin isotherm analyses calculated for the adsorption of MB, MG, and MV on P and AP from aqueous solutions. Equilibrium relationships between adsorbent and dyestuff were explained by adsorption isotherms. When the MB, MG, and MV dyestuffs were compared with P and AP, correlation coefficients ( $R^2$  value) and modified Langmuir, Freundlich, Scatchard, D-R, and Temkin isotherm models agreed with the experimental data (Fig. 7a, b). Therefore, it was seen that there was more than one adsorption mechanism. The suitability of the equilibrium curve for the modified Langmuir isotherm was studied, and  $q_m$  and  $K_{ML}$  were calculated from Eq. (3) and were given in Table 2.  $C_s$  is the saturation concentration of dye molecules in liquid phase (40,000 mg/L for MB, 60,000 mg/L for MG, and 33,000 mg/L for MV).  $K_{ML}$  is the equilibrium constants of modified Langmuir (Seifikar and Azizian 2019). The modified Langmuir isotherm was more applicable for dyestuff adsorption compared to other isotherm data. The maximum adsorption capacities of

dyestuff according to the modified Langmuir isotherm model were 6.64 mg/g-P/MB, 3.86 mg/g-P/MG, and 4.97 mg/g-P/MV and 104.1 mg/g-AP/MB, 74.6 mg/g-AP/MG, and 149.2 mg/g-AP/MV. According to  $q_m$  values, it was observed that the interest of MV dyestuff on P and AP was higher than MB and MG. The Freundlich equation of  $K_f$  and  $n$  values was calculated (Eq. (4)). The slope  $n$  measures the surface heterogeneity. The  $n$  values were found to be 1.60-AP/MB, 1.50-AP/MG, 1.61-AP/MV, 2.57-P/MB, 2.63-P/MG, and 2.93-P/MV, indicating that the adsorption of these values was favorable from 1 to 10. D-R isotherm parameters are given in Table 2. Adsorption energy ( $E_{ad}$ ) value was found to be  $> 8$  kJ/mol (Eq. (5)). When the  $E_{ad}$  value was higher than 8 kJ/mol, the sorption process was said to be predominant by chemical sorption. Temkin isotherm is shown in Fig. 7a, b; the related parameters are given in Table 2.  $B$  values were 19.49, 15.04, 28.58, 1.24, 0.79, and 0.95 kJ mol<sup>-1</sup> for AP/MB, AP/MG, AP/MV, P/MB, P/MG, and P/MV, respectively. Values higher than 8 indicated stronger cohesive forces in between AP and dyestuffs. However,

**Table 2** Adsorption isotherm parameters for removal of MG, MV, and MB

Model	Equation	Eq.	Ads.	Dye	Parameters for dye			Reference	
Modified Langmuir	$\frac{C_e}{q_e} = \frac{C_e}{K_{ML}q_m} + \frac{(K_{ML}-1)C_e}{K_{ML}q_m}$	(3)	AP	MB	$q_m$	104.1	$K_{ML}$	1100	$R^2$ Azizian et al. 2018
			AP	MG		74.6		1292	
			AP	MV		149.2		2381	
			P	MB		6.64		3003	
			P	MG		3.86		6089	
			P	MV		4.97		4417	
Freundlich	$1nq_e = 1nK_f + \frac{1}{n}1nC_e$	(4)	AP	MB	$K_f$		$n$	$R^2$	Freundlich 1906
			AP	MG		4.87		1.60	
			AP	MV		2.64		1.50	
			P	MG		12.22		1.61	
			P	MV		1.07		2.57	
			P			0.70		2.63	
D-R	$lnq_e = lnq_m - \beta \epsilon^2$	(5)	AP	MB	$X_m$		$K$	$E$	$R^2$ Dubinin and Radushkevich 1947
			AP	MG		$*10^{-3}$	0.0073	8.84	
			AP	MV		7.25	0.0072	8.33	
			P	MB		6.04	0.0058	9.29	
			P	MG		14.33	0.0038	11.47	
			P	MV		0.29	0.0039	11.32	
Temkin	$q_e = BlnK_t + BlnC_e$	(6)	AP	MB	$B$		$K_t$	$R^2$	Temkin and Pyzhev 1940
			AP	MG		19.49	0.41	0.959	
			AP	MV		15.04	0.28	0.971	
			P	MB		28.58	1.05	0.966	
			P	MG		1.24	1.14	0.969	
			P	MV		0.79	1.13	0.953	
Scatchard	$q_e/C_e = Q_sK_s - q_eK_s$	(7)	AP	MB	$Q_s$		$K_s$	$R^2$	Scatchard, 1949
			AP	MG		108.0	0.03	0.936	
			AP	MV		96.71	0.017	0.744	
			P	MB		188.5	0.059	0.956	
			P	MG		5.95	0.118	0.783	
			P	MV		3.89	0.101	0.872	
					4.90	0.150	0.843		



**Fig. 7** Langmuir, Freundlich, Dubinin-Radushkevich, Scatchard, and Temkin isotherms plot for the adsorption of MB, MG and MV onto P (a) and AP (b)

values less than 8 indicate weak interaction between P and dyestuffs (Anwar et al. 2010). For dyestuff adsorption, the Scatchard curve was plotted and  $Q_s$  and  $K_s$  constant values were obtained from Eq. (7) and are given in Table 2. Calculated  $R^2$  value was 0.99 and supports the appropriateness of modified Langmuir isotherms for P and AP. The results also show that the adsorption of MB, MG, and MV with P and AP takes place in a single-layer adsorption form.

### Kinetic models

In this step of the study, the kinetic behavior of the adsorption process was tried to be elucidated by using data of adsorption experiments carried out at different dye concentrations. In order to determine the adsorption rate and rate constants of MB, MG, and MV dyes with P and AP, pseudo-first and pseudo-second-order model equations were used. Kinetic models have been used to find the mechanism of adsorption and its potential rate-controlling step that includes mass transport and chemical reaction. The kinetic parameters calculated from the kinetic models are presented in Table 3. The adsorption graphs of the models examined are given in Additional file 1: Figure S1, and the correlation coefficients ( $R^2$ ) are given in Table 3. The pseudo-second-order kinetic model was used based on the following differential equation (Ho 2006; Azizian 2004), where  $k_2$

is the rate constant of pseudo-second-order adsorption ( $\text{g mg}^{-1} \text{ min}^{-1}$ ). The boundary condition  $q_t = 0$  at  $t = 0$  and the equation can be linearized as Eq. (8):

$$\frac{t}{q_t} = \frac{1}{k_2 q_e^2} + \frac{t}{q_e} \quad (8)$$

The rate constants are represented in Table 3. The equilibrium capacities calculated from pseudo-second-order model agreed closely with the capacities found from isotherm studies. The correlation coefficients ( $R^2$ ) obtained with the pseudo-second-order kinetic model are above 0.990. Hence, the pseudo-second-order model equation was accepted as a useful model for the kinetic studies, indicating the chemical adsorption is the rate-limiting step. Similar results are available in the literature (Thakur et al. 2016). In this model, it is acknowledged that there is a single-layer coating on the surface but it can also be an additional layer of physically adsorbed molecules (Theydan and Ahmed 2012).

### Thermodynamic studies

Thermodynamic parameters such as the free energy change ( $\Delta G^\circ$ ), enthalpy change ( $\Delta H^\circ$ ), and entropy

**Table 3** Comparison of the pseudo-first-order and pseudo-second-order adsorption rate constants and the calculated and experimental  $q_e$  values obtained at different initial dye concentrations

Adsorbent	Dye	$C_0$ (ppm)	$q_{e \text{ exp}}$	Pseudo-first-order			Pseudo-second-order		
				$k_1$	$q_e$	$R^2$	$k_2$	$q_e$	$R^2$
AP	MB	25	20.90	0.010	10.60	0.866	0.0031	20.83	0.999
	MB	50	35.87	0.013	16.06	0.799	0.0018	37.31	0.998
	MB	100	70.83	0.012	28.21	0.966	0.0016	70.92	0.999
AP	MG	25	16.90	0.0096	9.68	0.892	0.0031	16.89	0.995
	MG	50	30.87	0.0136	16.47	0.854	0.0016	32.68	0.996
	MG	100	49.83	0.0117	16.84	0.800	0.0025	50.00	0.999
AP	MV	25	24.00	0.0169	6.90	0.786	0.0049	24.75	0.999
	MV	50	46.87	0.0116	10.63	0.560	0.0024	47.85	0.997
	MV	100	89.00	0.0190	35.86	0.871	0.0006	96.15	0.990
P	MB	10	3.00	0.0066	2.12	0.955	0.0130	2.74	0.989
	MB	25	4.25	0.0102	3.39	0.988	0.0053	4.56	0.983
	MB	50	6.20	0.0075	4.52	0.921	0.0047	6.08	0.996
P	MG	10	2.59	0.0031	2.02	0.781	0.0181	1.71	0.996
	MG	25	3.87	0.0063	2.50	0.895	0.0142	3.39	0.977
	MG	50	4.83	0.0089	4.07	0.978	0.0037	5.17	0.965
P	MV	10	2.19	0.0091	1.28	0.867	0.0241	2.16	0.997
	MV	25	3.87	0.0080	2.44	0.865	0.0110	3.76	0.993
	MV	50	5.83	0.0097	4.65	0.956	0.0030	6.46	0.974

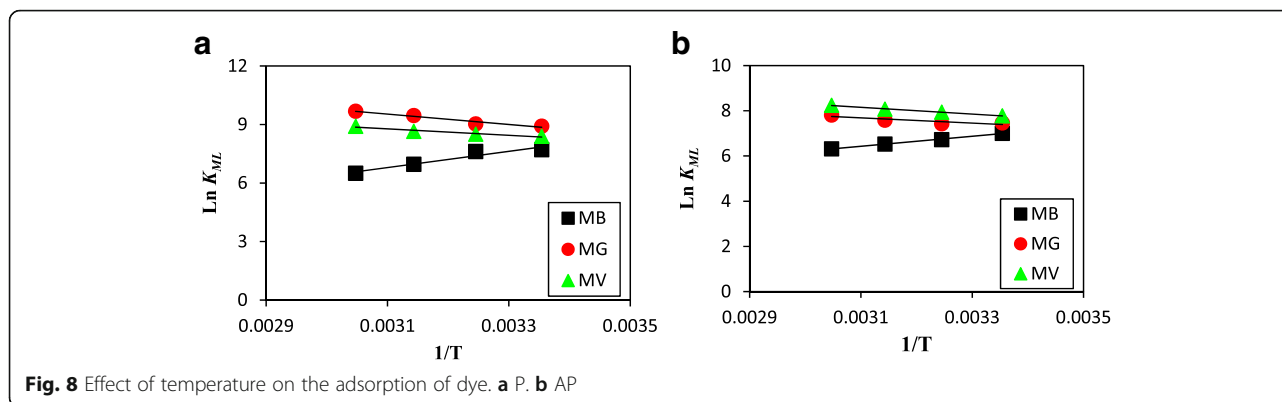


**Fig. 8** Effect of temperature on the adsorption of dye. **a** P. **b** AP

change ( $\Delta S^\circ$ ) of the adsorption processes were calculated from following Eqs. (9) and (10) (Azizian et al. 2018):

$$\ln q_e = \ln K_f + \frac{1}{n} \ln C_e \quad (9)$$

$$\ln K_{ML} = \frac{\Delta S^\circ}{R} - \frac{\Delta H^\circ}{RT} \quad (10)$$

Adsorption of MB, MG, and MV onto P and AP has definitely carried out different temperatures (25 °C, 35 °C, 45 °C, and 55 °C) for thermodynamic analysis (Fig. 8). The thermodynamic parameters including  $\Delta H^\circ$ ,  $\Delta S^\circ$ , and  $\Delta G^\circ$  for the adsorption of dyestuffs are calculated from plotted data, and the results are given in Table 4. The positive  $\Delta H^\circ$  values indicate that the adsorption is endothermic, and the negative is an exothermic process. The negative value of the standard entropy change reflects a decreased in the randomness at the solid-solution interface during the adsorption process, and the positive values of the irregularities increased. The  $\Delta S^\circ$  values are negative in the adsorption of MG and MV of both adsorbent. This is considered to be a reduction of irregularity in the solid-solution interface of the adsorption.  $\Delta S^\circ$  values are positive in the adsorption of MB; the water molecules on the surface of the adsorbents are replacing the dyestuff molecules with larger diameters. Therefore, a decreasing molecule in the environment is expressed as an increase in irregularity at the solid-solution interface since more

molecules of water (small diameter) will be added to the dye molecule. Negative values of  $\Delta G^\circ$  indicate the applicability of the method and that the adsorption is spontaneous. As seen from the results, with both P and AP, the adsorption of MB was exothermic and the other pores were endothermic.  $\Delta G^\circ$  is negative in three dye removal by AP, and the adsorption is spontaneous.

#### Comparison of cationic dyes adsorption with different adsorbents reported in literature

The maximum adsorption capacity  $q_m$  (mg/g) obtained for the beads is shown in Table 5. Compared to the other adsorbents used for the various dyestuffs reported in the literature, the AP obtained in this study can be used as potential adsorbent in various dyestuff removals. Of course, when comparing the chemical groups on the beads, the surface area of the beads, porous structure, and pH of the solution must be considered important parameters. Compared to the literature values, the adsorption capacity of the composites prepared in this study was found to be quite good. In addition, it has been observed that the composites prepared have better adsorption capacity compared to perlite, and therefore, our aim was to make composite.

The experimental results of our investigation revealed that AP has highest sorption capacity. Many workers have experimented various adsorbents for MB, MG, and MV dye adsorption. A comparison of the adsorbent

**Table 4** Thermodynamic parameters for dye adsorption onto P and AP

Adsorbent	Dye	$\Delta S^\circ$	$\Delta H^\circ$	$\Delta G^\circ$				$R^2$
				T = 298.15 K	T = 308.15 K	T = 318.15 K	T = 328.15 K	
AP	MB	-3.5	-18,427	-17,382	-17,347	-17,312	-17,277	0.997
AP	MG	117	17,152	-17,844	-19,017	-20,191	-21,365	0.993
AP	MV	107	12,531	-19,329	-20,397	-21,466	-22,534	0.996
P	MB	-74	-42,143	-20,052	-19,311	-18,570	-17,829	0.989
P	MG	164	27,277	-21,665	-23,306	-24,948	-26,589	0.990
P	MV	116	13,788	-20,782	-21,942	-23,101	-24,261	0.949

**Table 5** Adsorption capacities of various composites for the adsorption of dyes

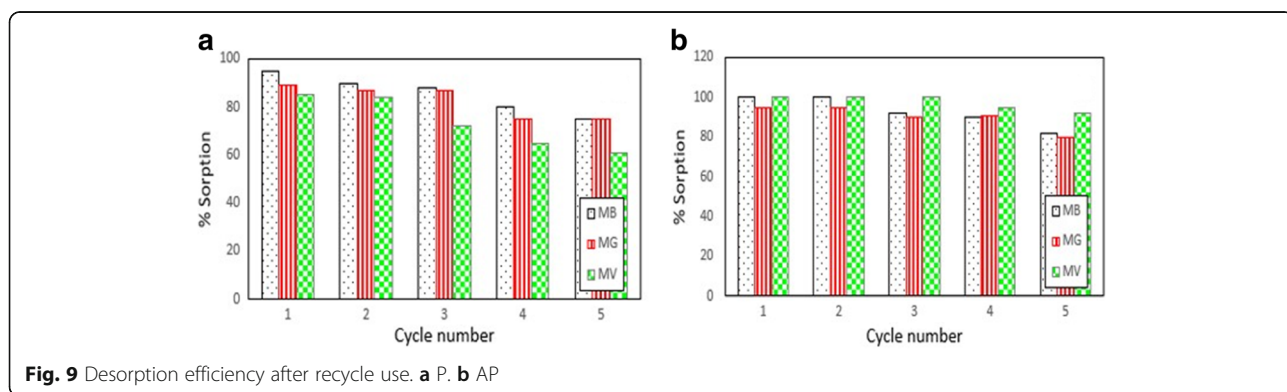
Adsorbent	Dyes	Adsorption capacities (mg/g)	Reference
Magnetic porous carbon	Methylene blue	61.65	Zhang et al. 2017
Chitin/clay microspheres	Methylene blue	152.2	Xu et al. 2018
Moroccan clay	Crystal violet	12.19	Miyah et al. 2017
Glutamic acid modified chitosan magnetic composite	Methylene blue	180	Yan et al. 2013
Modified activated carbon	Crystal violet	12.60	Hamidzadeh et al. 2015
Rice hull char	Methyl violet	48.7	Xu et al. 2011
Natural zeolite	Methylene blue	16.37	Han et al. 2009
Modified clay	Malachite green	40.48	Arellano-Cárdenas et al. 2013
Bentonite	Malachite green	7.716	Tahir and Rauf 2006
Kaoline	Methylene blue	13.99	Al-Futaisi et al. 2007
Superparamagnetic sodium alginate-coated Fe3O4 nanoparticles	Malachite green	47.84	Mohammadi et al. 2014
Carboxylate functionalized multi-walled carbon nanotubes	Malachite green	49.45	Sadegh et al. 2015
HNT-Fe3O4 composite	Methyl violet	20.04	Bonetto et al. 2015
Alginate coated perlite	Methylene blue	104.2	Present work
	Malachite green	74.63	Present work
	Methyl violet	149.3	Present work
Perlite	Methylene blue	6.65	Present work
	Malachite green	3.87	Present work
	Methyl violet	4.98	Present work

capacity with other adsorbents reported in literature is given in Table 5 and compared with P and AP. The experimental data of the present investigations are comparable with the reported values. The results indicated that the maximum adsorption capacity obtained in this study showed significantly higher dye adsorption capacities versus native adsorbent and comparable with composites.

**Desorption study**

To examine the possibility of recycling of the adsorbents, desorption was performed with 1.0 M HCl

solution as eluant. Regeneration is an important fact of the adsorption process; it can not only recover the dye-stuff removed from the aqueous phase but also lead to reusability of the adsorbent that employed in the adsorption process. This procedure makes the operation more useful, cheaper, and applicable. MB, MG, and MV dye-loaded P/AP was dried at 70 °C and placed in contact with 1.0 M HCl, and each mixture was constantly stirred for 24 h. Figure 9 shows the removal capacity of AP and the removal efficiency of MB, MG, and MV after using the same AP for several times. Maximum dyestuff desorption capacity was achieved using AP (95.65%).



Experimental results showed that produced AP and P displayed reasonable adsorption for repeated practical application.

## Conclusions

In this study, batch adsorption experiments for the uptake of MB, MG, and MV from aqueous solutions have been carried out using low-cost different adsorbents—P and AP. Adsorption is found to depend on pH, adsorbent dose, and contact time. The initial pH solution has a marked influence on the MB, MG, and MV adsorption performance. Equilibrium adsorption data were correlated with modified Langmuir, Freundlich, Scatchard, D-R, and Temkin adsorption isotherm equations. Isotherm studies revealed that modified Langmuir model has well described the equilibrium data of MB, MG, and MV for P and AP. The maximum adsorption capacities ( $q_m$ ) calculated with the Langmuir isotherm model were 6.64 mg/g-P/MB, 3.86 mg/g-P/MG, and 4.97 mg/g-P/MV and 104.1 mg/g-AP/MB, 74.6 mg/g-AP/MG, and 149.2 mg/g-AP/MV. Alginate coating has shown great promise in improving the MB, MG, and MV adsorption capacity of perlite. The pH effect of adsorption of MB, MG, and MV on the P and AP was investigated, and the best pH for all adsorbent was 6. The adsorption equilibrium was reached at about 1 h for AP. Kinetic data showed that the dynamic tendency of MB, MG, and MV adsorption could be defined by pseudo-second-order kinetic model. Thermodynamic calculations showed that the MB, MG, and MV dye adsorption with AP was spontaneous in nature. This study showed the high removal efficiency of AP for the removal of MB, MG, and MV from aqueous solutions.

## Additional file

**Additional file 1: Figure S1.** Kinetic models (pseudo-first-order kinetic model and pseudo-second-order kinetic model) for dye adsorption onto (a) P and (b) AP. (DOCX 45 kb)

## Abbreviations

AP: Alginate-coated perlite beads; MB: Methylene blue; MG: Malachite green; MV: Methyl violet; P: Perlite

## Acknowledgements

Not applicable

## Funding

Not applicable

## Availability of data and materials

Research data have been provided in the manuscript.

## Author's contributions

ŞP is the only author of the manuscript and the inventor of the software. Consequently, she contributed alone to this work. The author read and approved the final manuscript.

## Competing interests

The author declare that she has no competing interests.

## Publisher's note

Springer Nature remains neutral with regard to jurisdictional claims in published maps and institutional affiliations.

Received: 14 November 2018 Accepted: 4 January 2019

Published online: 17 January 2019

## References

- Abdelrahman EA. Synthesis of zeolite nanostructures from waste aluminum cans for efficient removal of malachite green dye from aqueous media. *J Mol Liq.* 2018;253:72–82.
- Abdelrahman EA, Hegazey RM. Utilization of waste aluminum cans in the fabrication of hydroxysodalite nanoparticles and their chitosan biopolymer composites for the removal of Ni (II) and Pb (II) ions from aqueous solutions: kinetic, equilibrium, and reusability studies. *Microchem J.* 2019;145:18–25.
- Abdelrahman EA, Tolan DA, Nassar MY. A tunable template-assisted hydrothermal synthesis of hydroxysodalite zeolite nanoparticles using various aliphatic organic acids for the removal of zinc (II) ions from aqueous media. *J Inorg Organomet Polym Mater.* 2018;1–19.
- Al-Futaisi A, Jamrah A, Al-Hanai R. Aspects of cationic dye molecule adsorption to polygorskite. *Desalination.* 2007;214(1–3):327–42.
- Anwar J, Shafique U, Salman M, Dar A, Anwar S. Removal of Pb (II) and Cd (II) from water by adsorption on peels of banana. *Bioresour Technol.* 2010; 101(6):1752–5.
- Arellano-Cárdenas S, López-Cortez S, Cornejo-Mazón M, Mares-Gutiérrez JC. Study of malachite green adsorption by organically modified clay using a batch method. *Appl Surf Sci.* 2013;280:74–8.
- Asadi S, Eris S, Azizian S. Alginate-based hydrogel beads as a biocompatible and efficient adsorbent for dye removal from aqueous solutions. *ACS Omega.* 2018;3:15140–8.
- Azizian S. Kinetic models of sorption: a theoretical analysis. *J Colloid Interface Sci.* 2004;276:47–52.
- Azizian S, Eris S, Wilson LD. Re-evaluation of the century-old Langmuir isotherm for modeling adsorption phenomena in solution. *Chem Phys.* 2018;513:99–104.
- Bentahar S, Dbik A, El Khomri M, El Messaoudi N, Lacherai A. Removal of a cationic dye from aqueous solution by natural clay. *Groundwater Sustainable Development.* 2018;6:255–62.
- Bonetto LR, Ferrarini F, De Marco C, Crespo JS, Guégan R, Giovanela M. Removal of methyl violet 2B dye from aqueous solution using a magnetic composite as an adsorbent. *J Water Process Eng.* 2015;6:11–20.
- Bouasla C, Samar MEH, Ismail F. Degradation of methyl violet 6B dye by the Fenton process. *Desalination.* 2010;254(1-3):35–41.
- Crini G. Non-conventional low-cost adsorbents for dye removal: a review. *Bioresour Technol.* 2006;97:1061–85.
- Crini G, Badot PM. Application of chitosan, a natural aminopolysaccharide, for dye removal from aqueous solutions by adsorption processes using batch studies: a review of recent literature. *Prog Polym Sci.* 2008;33(4):399–447.
- Dąbrowski A. Adsorption—from theory to practice. *Adv Colloid Interf Sci.* 2001; 93(1–3):135–224.
- Djebri N, Boutahala M, Chelali NE, Boukhalifa N, Zeroual L. Enhanced removal of cationic dye by calcium alginate/organobentonite beads: modeling, kinetics, equilibriums, thermodynamic and reusability studies. *Int J Biol Macromol.* 2016;92:1277–87.
- Dubin MM, Radushkevich LV. Equation of the characteristic curve of activated charcoal. *Proc Acad Sci Physical Chem Section.* 1947;55:331.
- Freundlich HMF. Over the adsorption in solution. *J Phys Chem.* 1906;57:385–471.
- Ghaedi M, Nasab AG, Khodadoust S, Rajabi M, Azizian S. Application of activated carbon as adsorbents for efficient removal of methylene blue: kinetics and equilibrium study. *J Ind Eng Chem.* 2014;20(4):2317–24.
- Gobi K, Mashitah MD, Vadivelu VM. Adsorptive removal of methylene blue using novel adsorbent from palm oil mill effluent waste activated sludge: equilibrium, thermodynamics and kinetic studies. *Chem Eng J.* 2011;171(3): 1246–52.
- Hamidzadeh S, Torabbeigi M, Shahtaheri SJ. Removal of crystal violet from water by magnetically modified activated carbon and nanomagnetic iron oxide. *J Environ Health Sci Eng.* 2015;13(1):8.

- Han R, Zhang J, Han P, Wang Y, Zhao Z, Tang M. Study of equilibrium, kinetic and thermodynamic parameters about methylene blue adsorption onto natural zeolite. *Chem Eng J*. 2009;145(3):496–504.
- Ho YS. Review of second-order models for adsorption systems. *J Hazard Mater*. 2006;B136:681–9.
- Langmuir I. The constitution and fundamental properties of solids and liquids. Part I. Solids. *J Am Chem Soc*. 1916;38(11):2221–95.
- Miyah Y, Lahrichi A, Idrissi M, Boujraf S, Taouda H, Zerrouq F. Assessment of adsorption kinetics for removal potential of crystal violet dye from aqueous solutions using Moroccan pyrophyllite. *J Assoc Arab Univ Basic Appl Sci*. 2017;23(1):20–8.
- Mohammadi A, Daemi H, Barikani M. Fast removal of malachite green dye using novel superparamagnetic sodium alginate-coated Fe<sub>3</sub>O<sub>4</sub> nanoparticles. *Int J Biol Macromol*. 2014;69:447–55.
- Nassar MY, Abdelrahman EA. Hydrothermal tuning of the morphology and crystallite size of zeolite nanostructures for simultaneous adsorption and photocatalytic degradation of methylene blue dye. *J Mol Liq*. 2017;242:364–74.
- Nassar MY, Abdelrahman EA, Aly AA, Mohamed TY. A facile synthesis of mordenite zeolite nanostructures for efficient bleaching of crude soybean oil and removal of methylene blue dye from aqueous media. *J Mol Liq*. 2017;248:302–13.
- Oussalah A, Boukerroui A, Aichour A, Djellouli B. Cationic and anionic dyes removal by low-cost hybrid alginate/natural bentonite composite beads: adsorption and reusability studies. *Int J Biol Macromol*. 2019;124:854–62.
- Papegowda PK, Syed AA. Isotherm, kinetic and thermodynamic studies on the removal of methylene blue dye from aqueous solution using saw palmetto spent. *Int J Environ Res*. 2017;11(1):91–8.
- Pehlivan E, Altun T, Parlayıcı S. Utilization of barley straws as biosorbents for Cu<sup>2+</sup> and Pb<sup>2+</sup> ions. *J Hazard Mater*. 2009;164(2–3):982–6.
- Puri C, Sumana G. Highly effective adsorption of crystal violet dye from contaminated water using graphene oxide intercalated montmorillonite nanocomposite. *Appl Clay Sci*. 2018;166:102–12.
- Sadegh H, Shahyari-ghoshekandi R, Agarwal S, Tyagi I, Asif M, Gupta VK. Microwave-assisted removal of malachite green by carboxylate functionalized multi-walled carbon nanotubes: kinetics and equilibrium study. *J Mol Liq*. 2015;206:151–8.
- Salleh MAM, Mahmoud DK, Karim WAWA, Idris A. Cationic and anionic dye adsorption by agricultural solid wastes: a comprehensive review. *Desalination*. 2011;280(1–3):1–13.
- Scatchard G. The attractions of proteins for small molecules and ions. *Ann N Y Acad Sci*. 1949;51:660–72.
- Seifikar F, Azizian S. A facile method for precipitating of dispersed carbon particles prepared by microwave heating and its application for dye removal. *J Mol Liq*. 2019;275:394–401.
- Tahir SS, Rauf N. Removal of a cationic dye from aqueous solutions by adsorption onto bentonite clay. *Chemosphere*. 2006;63(11):1842–8.
- Temkin MJ. Kinetics of ammonia synthesis on promoted iron catalysts. *Acta Physiochim URSS*. 1940;12:327–56.
- Temkin MJ, Pyzhev V. Recent modifications to Langmuir isotherms. *Acta Physiochim USSR*. 1940;12:217–22.
- Thakur S, Pandey S, Arotiba OA. Development of a sodium alginate-based organic/inorganic superabsorbent composite hydrogel for adsorption of methylene blue. *Carbohydr Polym*. 2016;153:34–46.
- Theydan SK, Ahmed MJ. Adsorption of methylene blue onto biomass-based activated carbon by FeCl<sub>3</sub> activation: equilibrium, kinetics, and thermodynamic studies. *J Anal Appl Pyrolysis*. 2012;97:116–22.
- Vega-Negron AL, Alamo-Nole L, Perales-Perez O, Gonzalez-Mederos AM, Jusino-Olivencia C, Roman-Velazquez FR. Simultaneous adsorption of cationic and anionic dyes by chitosan/cellulose beads for wastewaters treatment. *Int J Environ Res*. 2018;12(1):59–65.
- Xu R, Mao J, Peng N, Luo X, Chang C. Chitin/clay microspheres with hierarchical architecture for highly efficient removal of organic dyes. *Carbohydr Polym*. 2018;188:143–50.
- Xu RK, Xiao SC, Yuan JH, Zhao AZ. Adsorption of methyl violet from aqueous solutions by the biochars derived from crop residues. *Bioresour Technol*. 2011;102(22):10293–8.
- Yan H, Li H, Yang H, Li A, Cheng R. Removal of various cationic dyes from aqueous solutions using a kind of fully biodegradable magnetic composite microsphere. *Chem Eng J*. 2013;223:402–11.
- Yi FY, Zhu W, Dang S, Li JP, Wu D, Li YH, Sun ZM. Polyoxometalates-based heterometallic organic–inorganic hybrid materials for rapid adsorption and selective separation of methylene blue from aqueous solutions. *Chem Commun*. 2015;51(16):3336–9.
- Zhang H, Chen L, Li L, Yang Y, Liu X. Magnetic porous carbon microspheres synthesized by simultaneous activation and magnetization for removing methylene blue. *J Porous Mater*. 2017;24 (2):341–53.

Submit your manuscript to a SpringerOpen<sup>®</sup> journal and benefit from:

- Convenient online submission
- Rigorous peer review
- Open access: articles freely available online
- High visibility within the field
- Retaining the copyright to your article

Submit your next manuscript at ► [springeropen.com](https://www.springeropen.com)